Parametric study of semi-rigid composite connections with 3-D Finite element approach

Feng Fu D.Lam J.Q. Ye

School of Civil Engineering, University of Leeds, Leeds, LS2 9JT, UK

Abstract

This paper describes the 3-dimensional finite element modelling of composite connection with steel beams and precast hollow core slab. A finite element model to simulate the structural behaviour of the composite beam was described and was used to study the behaviour of a wide range of composite connections to gain a better understanding of the structural behaviour especially the moment-rotation characteristic of the connections. Parametric studies were carried out to investigate the structural behaviour with variations in: size of the beam, thickness of the endplate, thickness of column web, depth of precast hollow cored slab and stud spacing. Through the parametric study, the structural behaviour of the composite connection has been discussed in detail, recommendations for the design purpose has been made.

Keyword precast hollow core slab; finite element ; semi-rigid; composite connection

1. Introduction

Although the use of precast hollow core slabs dates back to the 1940s, research on composite construction incorporating steel beams with precast hollow core slabs is relatively new. Recently, there is an increasing interest from the industry to imbed longitudinal bars across the column edge to form the composite connections. As most composite connections used in steel frames actually exhibit semi-rigid behavior, so the study on the semi-rigid composite connections with the precast hollow core slab is important for the future applications in the design practice. In the study of this new

type of connections, the relevant properties of connections are moment capacity, rotational stiffness and rotational capacity. These parameters can be defined using the moment-rotation response However, as a newly developed technology, the moment-rotation characteristic for this kind of connection is unclear. The most effective method to obtain the moment-rotation response is through the full scale tests. 8 full scale tests were firstly conducted by Fu and Lam [1]. In their tests, different parameters were studied, which are the stud spacing, degree of shear connection, thickness of the slab and area of the longitudinal bar. The full moment-rotation curves are obtained. Although the experimental tests provide reliable results that can describe the behaviour of the beam-to-column connections, due to the large number of variables and potential modes of failure associated with this type of connections, it is unlikely that all aspects of the problem have been thoroughly examined. Use of finite element modelling could explore large number of variables and potential failure modes, which could complement the experimental studies. Therefore, the parametric study through numerical approach is an extremely powerful way to developing a full understanding of complex structural behaviour of the connections.

For the modelling of the composite constructions, limited research has been done so far. Ayoub and Filippou [2] presented an inelastic beam element for the analysis of steel–concrete composite girders with partial composite action under monotonic and cyclic loads. This element is derived from a two-field mixed formulation. Fiber discretization of section and hysteric material models for the constituent materials are used to achieve the nonlinear response. Sebastian and McConnel [3] developed another beam element with layered steel beam and layered concrete slab for the analysis of steel–concrete composite girders. In this element, they also included the modeling of profiled steel sheeting. A specialized stub element with an empirical

nonlinear shear force–slip relationship is used at the concrete slab–steel beam interface to permit the modeling of either full or partial shear connector action. K.Baskar et.al [4] built up a 3-D FE model using ABAQUS to analyze the steel-concrete composite plate girders under negative bending and shear loading. The composite girders are modeled with shear studs .The deck slab is modeled with 3D solid elements. In order to overcome the convergence problem of the concrete material under the negative bending conditions deferent material properties have been tried. The successful material adopted is the CAST IRON MODEL and ELASTIC–PLASTIC MODEL. Ahmed[5] proposed a 2-D model for the analysis of composite connections and composite frames using ABAQUS. in order to overcome the convergence problem of the concrete slab simulation, they ignored the concrete slab under negative bending and analyzed the steel beam with multipoint constraint to behave like a composite girder.

2. 3-D finite element model

A three-dimensional finite element model created by Fu et al [6] using ABAQUS package [7] to conduct the parametric of the composite connections. As shown in Fig.1,. it replicates a composite connection from the experimental program of Fu and Lam [1]. The connection consists of one 254×254×167UC column beams connected with 2 457×191×89 UB beams using 10 mm thick flush end-plates and 4 M20 bolts. Due to the symmetry of cruciform arrangement tests only one side of the tests has been simulated. The boundary condition and method of loading adopted in the finite element analysis followed closely those used in the tests. Material nonlinearity was included in the finite element model by specifying a stress-strain curve in terms of the true stress and plastic strain. The engineering stresses and strains obtained from the

coupon tests of Fu et al [1] were converted into true stresses and strains for this purpose. Contact between all parts is explicitly modeled. The complex interaction between the surfaces of the end-plate and column flange, bolt head/nut and end-plate, were modeled with the node-to-node contact elements.

Different element types have been tried in order to choose the suitable element to simulate the behaviour of the composite connections. 3-D continuum elements are found to be more efficient in modelling all the component of the connection. As stated in the ABAQUS manual, the fully integrated, second-order, solid elements available in ABAQUS/Standard are very susceptible to volumetric locking when modelling incompressible material behaviour and, therefore, should not be used in elastic-plastic simulations. The fully integrated, first-order, solid elements in ABAQUS/Standard do not suffer from volumetric locking because ABAQUS actually uses a constant volume strain in these elements. Thus, they can be used safely in plasticity problems. Reduced-integration solid elements have fewer integration points at which the incompressibility constraints must be satisfied. Therefore, they are not ver-constrained and can be used for most elastic-plastic simulations. Trial error simulation has been made by the author, finally C3D8R element with reduced integration (1 Gauss point) has been chosen for the simulation of all the component in the model as it can provide more accurate result than the other elements. The efficiency of this type of the elements has been verified by the test results.

Different mesh sizes have been examined as well to determine reasonable mesh that provides both accurate results with less computational time. The exam results show that, if the mesh is too coarse (like that less than 20 elements along the 2-direction in the steel column flange), convergence problem will be caused as the contact element was used between the column flange and the endplate surface. However, if the mesh

is too fine, (like more than 50 elements along the 2-direction), the computational time is excessive.The mesh selected is shown in Fig.1. for the steel beams, the web is divided into 39 elements along 3-direction, 24 elements along 2-direction and 2 elements along 1-direction. The steel flange is divided into 39 elements along 3-direction, 9 elements along 2-direction, 1 element along 1 direction. For the steel column, the web is divided into 5 elements along 3-direction, 30 elements along 2-direction and 1 element along 1-direction; the flange is divided into 1 element along 3-direction, 30 elements along 2-direction and 5 elements along 1-direction. For the slab, it is divided into 49 elements along 3-direction, 7 elements along 2-direction and 5 elements along 1-direction.

For the boundary conditions, all concrete notes, longitudinal bar nodes which lie on the symmetry surface are restricted as fixed because of symmetry. The bottom of the column was defined as fixed. The load was applied at the end of the beam as shown in Fig.1 in increments using the modified RIKS method available in the ABAQUS library.

The structural steel components such as steel beams, steel column, stud and bolt are modelled as an elastic-plastic material in both tension and compression. Strains in compression and tension are the same. With *ELASTIC and *PLASTIC option, the yield and ultimate tensile strength of the steel beam is obtained firstly from the results of the coupon tests of Fu et al [1], and then converted into the ture stress and plastic strain with appropriate input format for ABAQUS. For the elastic part of the stress-strain curve, the value of the Young's modulus and the Poisson's ratio of the concrete are determined according to BS 5950[8], the value is 2.06×10^5 N/mm^2 and 0.3 respectively.

The mechanism of the bolted endplate connection is that the forces between the members are transferred through friction due to clamping between the members caused by the pretension force of the bolts. Many different approaches have been used by the researchers in the past to simulate the bolt pretension force, bolt – endplate interface, and bolt – column flange interface but most of them are fairly complicated. Here, a new technique is proposed by the authors to model the interface. To simulate the bolted endplate connections, the relationship between the column flange and the endplate is simulated using small-sliding contact. the pressure between the two faces, the normal contact pressure-overclosure relationships between two faces are chosen as hard. The friction between the endplate and the column was ignored. As shown in Fig.2, the shanks of the bolts were modelled as prismatic, having a diameter equal to the nominal bolt diameter of 20 mm. The details of the threads on the shank were neglected. A circular bolt head model that circumscribes the original shape and size of the M8.8 bolt was employed. Circular nuts were also modelled with the original size of the nut. Both the head and the nuts are directly connected to the shank. The washers and thread are not modelled. The nodes within each bolt head area on the bolted end plate are assumed to have the same displacements in the finite element models. The nodes of the inner layer of elements on both the edge plate and the end plate were paired up and constrained using the “TIE” option provided by ABAQUS [7]. With such an arrangement, both translational and rotational degrees of freedom of the tied nodes have the same displacement values during the deformation process. The same arrangement is made to simulate the interaction between the nut and the column flange as well. The contact bearing interaction between the shank and the bolts hole are neglected. By eliminating the simulation of the bolt pretension this model represents a dramatic reduction in the computational cost such as the numbers of element and the computing time.

Through the bond interactions between the concrete and the longitudinal bar, the shear force is transferred to the longitudinal bar. This composite construction is simulated as shown in Fig.3. in Fig.3, a discrete reinforced concrete slab model was built, both the slab and the reinforced steel is modelled by C3D8R 3-D solid element. The connectivity between a concrete node and a reinforcing steel node is achieved by using the *TIE option. The bond slip between the concrete and the slab is ignored.

The longitudinal shear force is transferred to the concrete by dowel action of the connector, which means that the connector is compressing the slab. The tests result of Fu et al [1] show that, the front side of the stud is in compressing, however, the back of the stud is in tension and the stud is separating from the concrete slabs.This mechanism is shown in Fig 4. Therefore, in the simulation only the nodes of the studs at the front side are connected to the nodes of the concrete slab with rigid connection using *TIE options and the other nodes of the studs are detached to the surrounding concrete nodes.

For the studs, to simplify the mesh, it is simulated with rectangular section with converted cross-sectional area of the actual studs used in the tests and the stud head is not modelled. The weld between the stud and the steel beam is not modelled,the node of the stud is directly connected with the steel beam. in the simulation only the node of the studs at the front side are connected to the concrete slab node and the other nodes of the studs are detached with the surrounding concrete nodes.

It was observed during the tests of Fu et.al [1] that the slab-to-steel beam friction was considered negligible and so has been ignored in the modelling. For the numerical simulation, the steel beam and the slab are considered to act without any connection

or contact. They are working compositely only through the connection of the shear studs.

Tests result shows that, in the hogging moment regions, the concrete slab is mainly under tension except that the area around the front of the shear studs as shown in Fig.3 the concrete is in compression, through this compression, the longitudinal shear force is transfered between the shear stud and the concrete slab. However, the convergence problem of ABAQUS to simulate the concrete material after cracking is reported by the authors, Ahmed [5] and K.Baskar et.al [4]. In order to overcome this problem, a simplified elastic-plastic material model was adopted here to simulate the concrete slab. As shown in Fig.5, it is assumed that the concrete behaves as a linear-elastic material up to the yield stress. Perfect plasticity is obtained when reaching the yield stress.The option (*PLASTIC) is used to specify the plastic part of the material model that use the von mises yield surface. For the elastic part of the stress-strain curve, the value of the Young's modulus and the Poisson's ratio of the concrete are determined according to EC4[9], value adopted is 3.5×10^4N/mm^2 and 0.2. For the plastic part, it is required to identify the yield stress. 2 different values are adopted in different area of the slab. The main area of the concrete slab (as shown in Fig. 3) is defined with the ultimate tensile stress f_t which is obtained from the indirect tensile test of Fu and Lam [1]. As shown in Fig.3, an area with $4\times$d length and 1.5 d width and the same height of the stud in the compressive side of the stud is defined with the yield stress 0.8 f_{cu} which is obtained from concrete cube tests. The compressive strain is given as 0.002 με. In this model, only in-situ concrete infill was modelled. The precast slab and the transverse bar are not modelled. The reason for this simplification is that the test results show that during the test, the strain reading of the transverse bar was quite small and remained elastic. So, the transverse bar has little effect on the

connection capacity. The effective width of the composite connection is taken as the width of the in-situ concrete infill and the precast hollowcore slabs are ignored.

3.Validation of proposed model

To validate the accuracy of the model, the FE analysis results are compared with the full scale test results of Fu et al [1]. Comparisons have been made for moment-rotation curve, moment-beam bottom flange strain curve, moment-slip curve and moment-rebar strain curves.The comparison results are shown in Figs.6-10. It can be seen that the numerical results have good agreement with the tests results. The last point represents the maximum rotation that can be reached up to the beginning of the failure. The model can accurately simulate the initial stiffness of the moment-rotation curve as in the simulation, the actual Young's modulus and the Poisson's ratio of concrete material were chosen. For the plastic part of the curve, the modelling result is slightly higher.This is because, the concrete tension model ignores the loss of conrete strength after the concrete reaches the ultimate tensile stress. After cracking the concrete still contributes to the moment capacity of the connection. However, the difference between the modelling results and the tests results are slight. The reason is that the longitudinal rebars yield quickly after the concrete reaches the ultimate tensile strength. Therefore, the contribution of the concrete to the moment capacity is quite small. In other words, the contribution of the concrete slab is limited by the yielding of the longitudinal bars. To verify this, the stress and the strain of the concrete slab element were extracted from the modelling results and converted back into Engineering stress and strain, the resulting relationship is shown in Fig. 11. It can be seen that, the stress in the concrete dropped off quickly after reaches the ultimate tensile stress due to the failure of the longitudinal bars yielding.The model also

predicts a larger rotation capacity. The discrepancy is because in the simulation, perfect bond interface between the steel rebars and the concrete slab has been presumed and the bond slip has been ignored. The tension stiffening effect of the concrete is also ignored. Therefore, after the slab is cracked, the connection between the steel rebasr and the slab is maintained in the model, though due to the tension stiffening effect, the embedded reinforcement has a lower overall ductility than bare reinforcement.

4. Parametric study of the composite connections

To better understand the structural behaviour of the joint, it is important to investigate the joints with systematic parametric studies. Table 1 shows the different parameters selected for FE analysis. Only one variable was changed at one group so as to asses its effect clearly. They are considered to be the most influential factors for the composite connections.

4.1 Effect of shear stud spacing

In oder to investigate the effect of the different stud spacing, 4 models has been built with different first stud spacing and stud number. As shown in Fig.12-15. Model CJ1 has 7 studs with the distance between the column flange and the first stud of 235mm, and the stud spacing is 300 mm. In model CJ1-6studs, the first stud of CJ1 has been removed. In model CJ1-5 studs, the first 2 studs of CJ1 has been removed. In model CJ1-4 studs, the first 3 studs of CJ1 were removed. The first stud spacing is shown in Table 2.All the other conditions are kept the same as CJ1. Fig.16 and Table 2 is the comparison of the moment-rotation curve for these 4 models. It can be seen that, there is no much difference in the moment capacity. This is because that, as long as the shear stud can provide the enough longitudinal shear force for the full mobilization of

the longitudinal bar, the tensile forces of the longitudinal bar are same, therefore there is little difference of the moment capacity. The rotation capacity increased as the first stud spacing increased. As discussed from the test result of Fu et al [1] that the effective moblization length of the longitudinal bar is between the column flange and the second stud, It can be seen from Fig.12 and Fig.13 the effective plastification length of 'reinforcement in tension' for model CJ1 and CJ1-6studs are within the first two stud, as the von mise stress in this area is much higher than the remaining area. As the length of CJ1-6studs is longer than CJ1, large rotation is observed. For model CJ1-5 studs and model CJ1-4 studs the studs has been placed over 800 mm distance away from the column flange, however the rotation capacities did not increased much in comparison with CJ1-6 studs. The test results of Helmut B, HansJ.K [10], Schafer and Kuhlmann [11] show that placing the studs further away from the column flange will result larger rotation capacity. It can be seen from Fig.14 and Fig.15 that, when the first stud spacing is increased to some limit, as over 800mm, the stress of the longitudinal steel bar is not uniform within the range from the column flange to the second stud, the high stress is concentrate within some certain length,The modelling result also shows that there is a slightly reduction of moment capacity, Therefore the rotation capacity could not increase further.

4.2 Effect of endplate thickness

Four endplate thickness 5mm,10mm,15mm 20mm were modelled respectively. The comparison result was shown in Fig.17 and table 3. Figs.18-21 are the four models at the failure. It can be seen that when the endplate thickness was decreased to 5mm, low moment capacity and rotation capacity were achieved. The mode of failure of model endplate 05 is due to the yielding of the end plate as shown in Fig.18, which caused the brittle failure of the connections. It is also shown that the thickness of the

endplate has great influence on the initial rotation stiffness of the connections, as the thickness increase from 5mm to 15mm, the initial stiffness increase, but when the thickness is greater than 15 mm, little difference was observed between the Moment-rotation curve of endplate15 and endplate20. The reason for this is that as the thickness of the endplate increased to certain thickness, the strength of the bolt become the influential factors, most area of the endplate remain elastic and the bolt will yield first. This permits higher tensile forces in the bolt which will increase the bending moment. However, as shown in Fig.20 and Fig.21,the brittle bolt failure was observed when the endplate increased to 15 mm and 20 mm, which caused the low rotation capacity as the brittle failure of the bolt stop the elongation of the longitudinal bar and therefore decrease the rotation capacity of the rotation. as the thickness of the plate increased, the mode of failure was changed from complete yielding of the flange (model CJ1) to bolt fracture with flange yielding (Endplate 15) and to bolt fracture (Endplate 20). EC3-part1.8 [12]has named this 3 mode of failure of bolted endplate with mode 1, mode 2 and mode 3 respectively. From above discussion, it is suggested that for the endplate in bending, it is necessary to limit the thickness of the endplate in order to avoid brittle failure of the bolts and to obtain ductile joints by yielding of the endplate in bending. If mode 1 failure does not occur, the connection may not have guaranteed ductility compatible with the extension of the reinforcement at the required rotation of the connection. And the endplate should also have certain thickness to avoid the brittle failure of the endplate itself.

4.3 Effect of different size of the steel beam

The modelling result are shown in Fig.22 and Table 4. Fig.23 is case 457×191×89 UB at failure, it can be seen that, as large beam size is chosen, the maximum stress of the bottom flange is only 213N/mm^2 still in the elastic range. The mode of failure is the yielding of the longitudinal bar. Fig.24 is case 406×140×39UB at failure, the mode

of the failure is still the yielding of the longitudinal bar. However, as a smaller beam size is used, the bottom flange yielding as well as that the yielding of the web is observed.Compared with the model 457×191×89 UB, the moment capacity of case 406×140×39 UB is reduced as smaller size beam has been chosen. The higher rotation capacity was result due to the deformation of the steel web.For the case 254×146×31UB, as the size of the steel beam is decreased further, another type of model of failure is observed, it is the local buckling of the bottom beam flange (as shown in Fig.25). The connection failed with low moment capacity and low rotation capacity. It can be seen that , for these three models, although same amount of the longitudinal steel bar were chosen, as smaller size beam were chosen, the modelling results were different. The tests result analysis from Fu et al [1] shows that with the heavy steel beams, higher amount of the longitudinal bar will cause the higher moment capacity and the rotation capacity. However, the failure of the steel components can prevented the specimen from attaining higher moment and rotation capacity. Therefore the reinforcement in the concrete slab must be carefully selected to commensurate with the local of the compression components, especially beam bottom flange compression resistance.

4.4 Effect of different column web thickness

To study the effect of the column web thickness on the behaviour of the composite connection, A small column size UC 203×203×46 was chosen in order to better investigate the effect of the column web thickness. and beam UB 406×140×139 were chosen for all the three models. The test results are shown in Fig.26 and table 5. In the result the rotation of the column is included to show the effect of the column web thickness, therefore the rotation of the three connection are greater. It is found from the modelling results that as the thickness of the web decreased the moment capacity decreased, the initial stiffness decreased and the rotation capacity increased. From the

comparison of the moment-rotation curve it can be seen that model web144 and web72 there is no obvious difference . As shown in Fig.27, for model web36 , a new mode of failure has been observed, it is the buckling of the column web, at the state of the failure, the ultimate stress of the column web obtained the ultimate strength of the steel 524 (N/mm^2) .The buckling of the column web caused low moment capacity. This is because that, the reduction of the thickness of the web reduce the compression capacity of the column web and reduced the compressive force at the interface of the beam and the column. Therefore the tensile forces in the longitudinal bar could not increase any further. The large deformation of the column greatly influence the rotation behaviour of the connection. And the deformation of the unstiffened connection is so large that the safety of structure need to be carefully check, therefore it is suggested that heavy column and stiffener on the beam to be used in the composite frame design. As the web thickness decreased, the rotation stiffness decreased. A stiffened column will provide better stiffness for the connection. The mechanical web stiffening may be considered to prevent premature buckling failure and retain high stiffness and ductility.

4.5 Effect of depth of the slab

The modelling result are shown in Fig.28 and Table 6. When the thickness increased, the moment capacity of has been increased distinctly This is to be expected as an increase in thickness of slab would raise the neutral axis of the composite beam, hence increasing the lever arm of the section. The failure model of this two models is the fracture of the longitudinal bar.

5.Conclusion

It can be concluded that the proposed 3-D FE modelling can accurately represent all the main features of the behaviour of composite endplate connections, it offers a reliable and very cost-effective alternative to laboratory testing as a way of generating results. Different variables have been studied on their influence on the structural behaviour of the connection, below findings are concluded:

1. Increased thickness of the endplate allows more tensile force in the bolts which increases the moment capacity, but the increase is not very significant and will cause brittle failure of the bolts with low rotation capacity of the connection. It is suggested that for the endplate in bending, it is necessary to limit the thickness of the endplate in order to avoid brittle failure of the bolts and to obtain ductile joints by yielding of the endplate in bending. And the endplate should also have certain thickness to avoid the brittle failure of the endplate itself.

2. Beyond certain limits imposed by the compression capacity of the beam flange and beam web and column web, further increases the amount of longitudinal bar are not possible to increase the moment and the rotation capacity of the connections. A very high reinforcement ratio can lead to a low rotation capacity.

3. Reduced thickness of beam flange leads to the buckling of the bottom flange, and higher web compression.

4. The buckling or bearing resistance of the column web may limit the maximum compression force that can be transferred. Heavy column Web stiffeners may be required for composite connections with a high percentage of slab reinforcement, leading to a greater compression transfer at the bottom flange.

5. Three different types of failure mode has been observed, rebar failure, the local bucking of the bottom beam flange and the distortion of the column.

6. Putting studs far away from column flange will increase the rotation capacity when the first stud spacing is over 700, it is not significant. The stud spacing has little effect on the moment capacity of the connection.

7. Increasing the slab thickness will increase the moment capacity of the connection.

8. Symmetry has been assumed in the modelling.However, in practice the unintentional asymmetry in material properties that structures can show may influence behaviour under load. This influence may be suggested as a topic for further study.

References

[1] Fu F. and Lam D. Experimental Study on Semi-Rigid Composite Joints with Steel Beams and Precast Hollowcore Slabs, Journal of Constructional Steel Research, (in press, to be published in Vol. 62,issue 8,2006, pp 771-782.)

[2] Ayoub. A., and Filippou. F. (2000). "Mixed formulation of nonlinear steel—concrete composite beam element." J. Struct. Eng. 126(3). 371-381.

[3] Sebastian, W. M., and McConnel. R. E. (2000). "Nonlinear FE analysis of steel-concrete composite structures." J. Struct. Eni;., 126(6), 662-674.

[4] Baskar K., Shanmugam N.E., Thevendran V (1996) Finite-element analysis of steel-concrete composite plate girder, Vol.128, No.9

[5]Ahmed, B Numerical Modelling of Semi-rigid Composite Joints, Ph.D. thesis,1996, University of Nottingham,U.K.

[6] Fu.F, Lam.D Ye J.Q. Modelling semi-rigid composite joints with precast hollowcore slabs in hogging moment region, (under review)

[7]ABAQUS theory manual, version 6.4. (2003) Hibbitt, K-arlsson and Sorensen. Inc.. Pawtucket, R.I.

[8]BS5950, Part 3-1, 'Structural use of steelwork in building: Code of practice for design of simple and continuous composite beams', British Standards Institution, London, 1990.

[9]Eurocode 4, Design of composite steel and concrete structures—Part 1.1 General rules and rules for buildings, ENV 1994-1-1:1992

[10]Helmut B, Hans J.K Behaviour of composite joints and their influence on semi-continuous composite beams, 1996, Composite construction in steel and concrete-III, Proc., Engineering Foundation Conf., ASCE, New York

[11]Schafer M. and Kuhlmann U., Innovative sway frames with partial-strength composite joints, 5th international PhD Symposium in Civil Engineering, Walraven, Blaauwendraad, Scarpas & Snijder (eds), 2004 Taylor & Francis Group, London

[12]Eurocode 3, Design of steel structures — Part 1.8 Design for joints, Joints in building frames, BS EN 1993-1-8:2005

Tables

Table 1 Values of parameters selected for parametric studies

Variable	Range of variable selected
Spacing of shear stud	235mm,535mm,835mm,1135mm
Endplate thickness	5mm, 10mm, 15mm, 20mm,
Size of steel beam	457×191×89 UB, 406×140×39UB, 254×146×31UB
Column web	3.6mm, 7.2 mm, 14.4 mm,
Precast slab thickness	150mm , 250mm, 400mm,

Table 2 Comparison of the modelling result

	First stud spacing	Moment capacity(kN.m)	Rotation capacity(Mrad)
CJ1	235 mm	52.9	440.5

CJ1-6studs	535 mm	55.98	425.6
CJ1-5studs	835 mm	56.7	416.5
CJ1-4studs	1135 mm	54.98	409

Table 3 Modelling result

Model name	Endplate thickness (mm)	Moment (kN.m)	Rotation	Mode of failure
Endplate05	5	185.5	11	B
Endplate10	10	406.4	38.3	A
Endplate15	15	420.9	22.3	B&C
Endplate20	20	429.8	23.6	C

Note: A. Fracture of longitudinal steel bar , B Endplate yielding, C bolt fracture

Table 4 Modelling result

Steel beam	Moment (kN.m)	Rotation (Mrad)	Maximun bottom flange stress (N/mm^2)	Mode of failure
UB 457×191×89	402	33.9	213	A
UB406×140×39	353	48.9	463	A
UC254×146×31	172	12	386	B

Note: A. Fracture of longitudinal steel bar B Local buckling of the bottom beam flange

Table5 Modelling result

	Moment (kN.m)	Rotation (Mrad)	Mode of failure

Web144	377	64.6	rebar
Web72	372	66.4	rebar
Web36	347	74.2	Column web buckling

Table 6 Modeling result

	Slab thickness (mm)	Moment(kN.m)	Rotation(Mrad)
CJ8	250	475.8	46.12
CJ8-150	150	428	61.9
CJ8-400	400	570	39.19

Figures

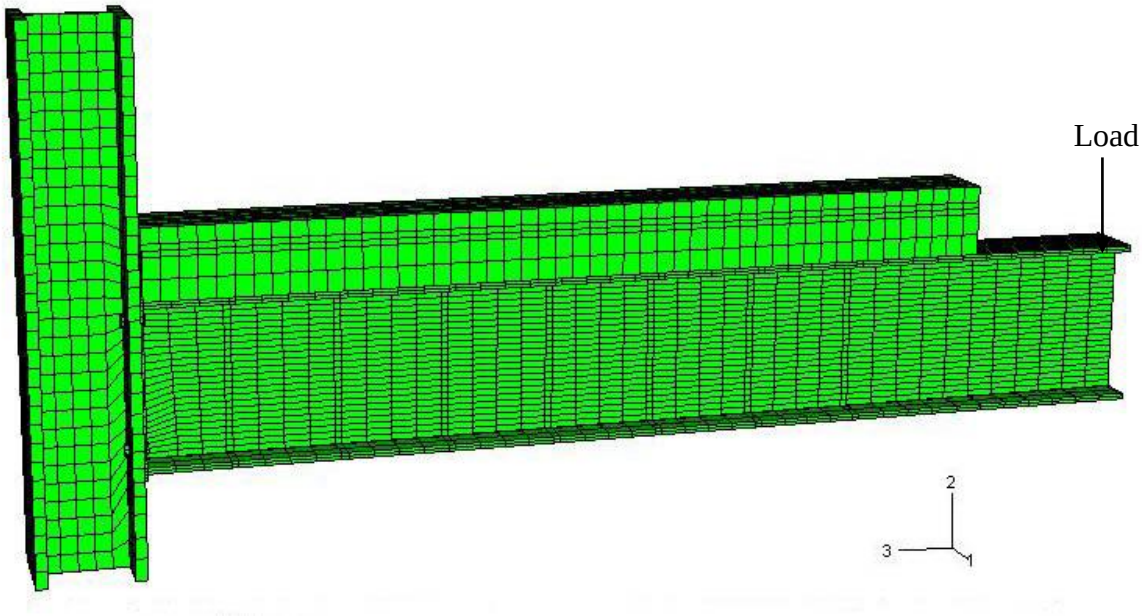

Fig 1 3-D finite element model of composite connection

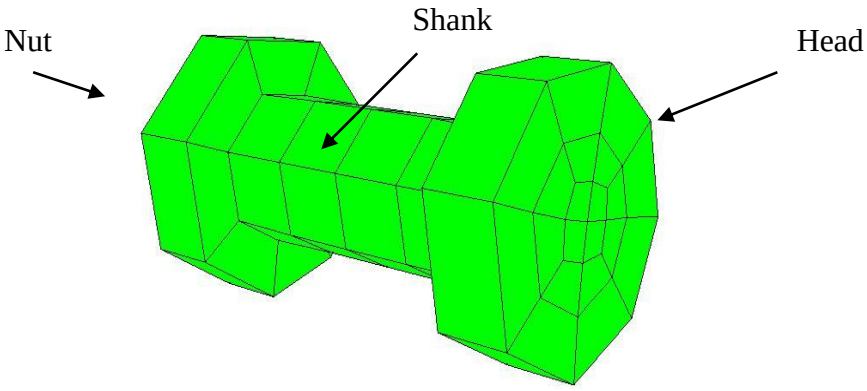

Fig. 2 3-D solid bolt model

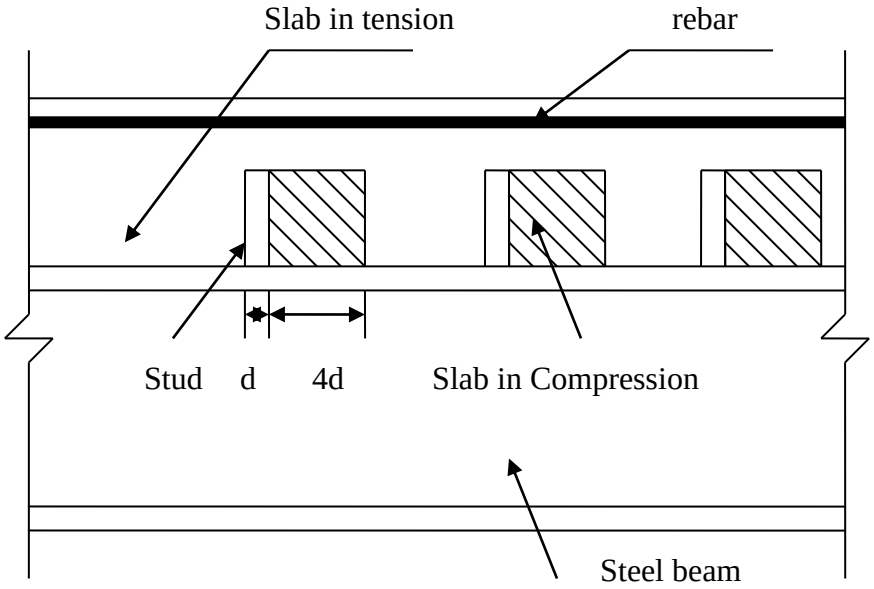

Fig 3 the composte construction model

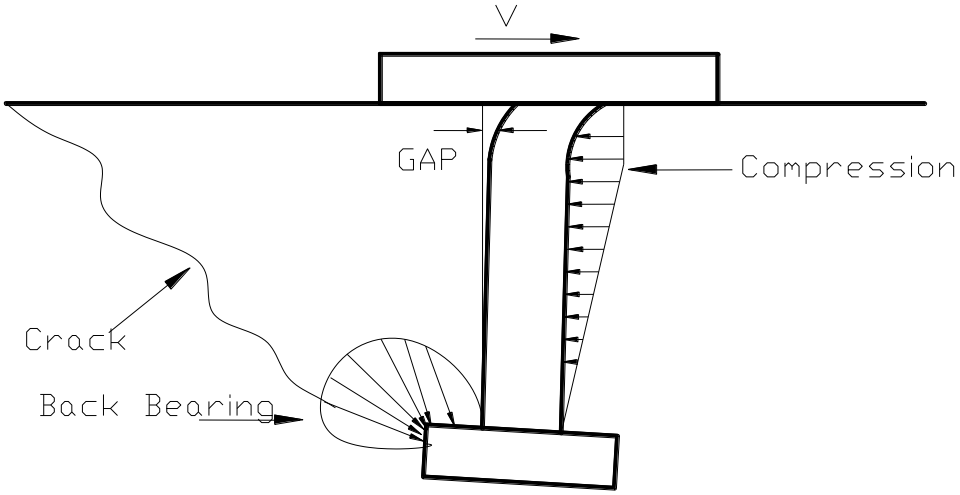

Fig 4 Deformation of shear stud in a concrete member

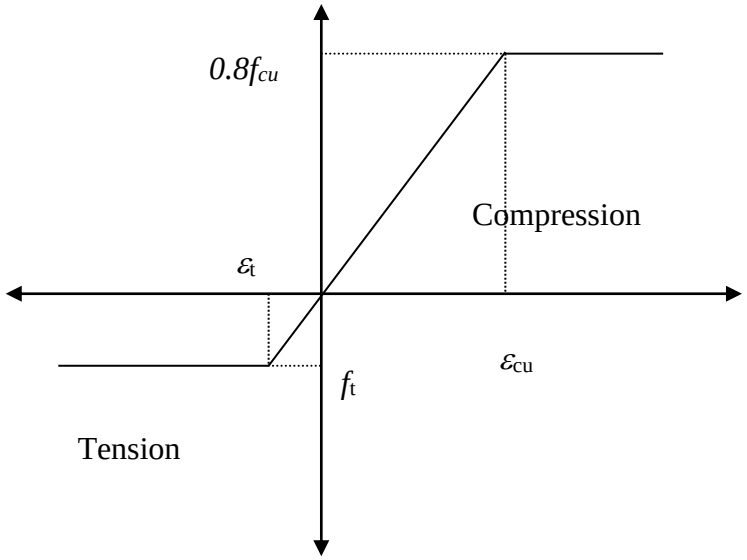

Fig 5 Elastic-plastic material model for concrete simulation

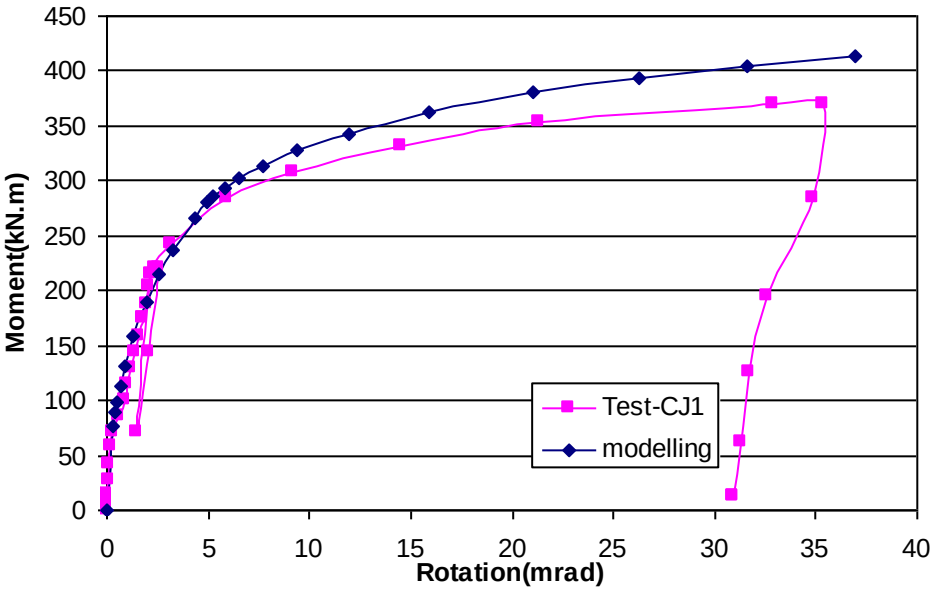

Fig. 6 Moment vs. rotation curves for test CJ1 and FE-solution

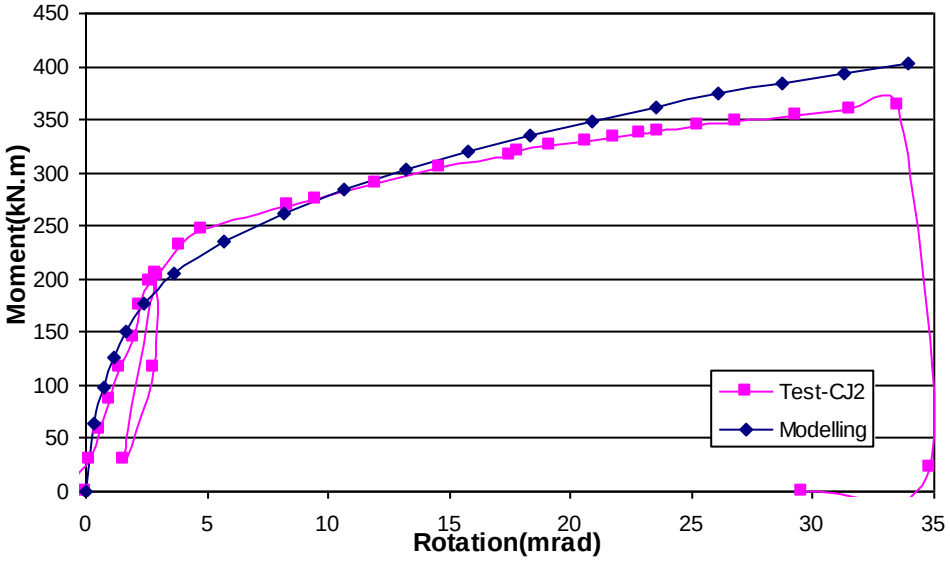

Fig. 7 Moment vs. rotation curves test CJ2 and FE-solution

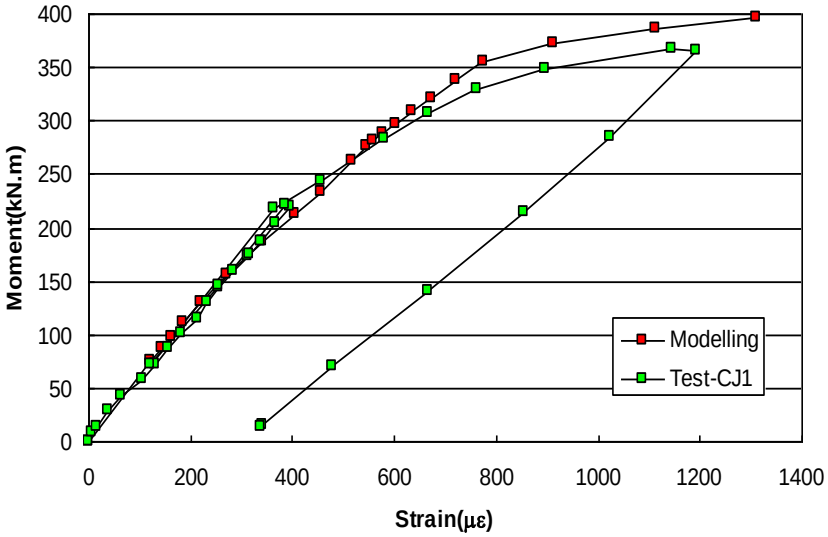

Fig 8 Comparison of moment-beam bottom flange strain curves for CJ1

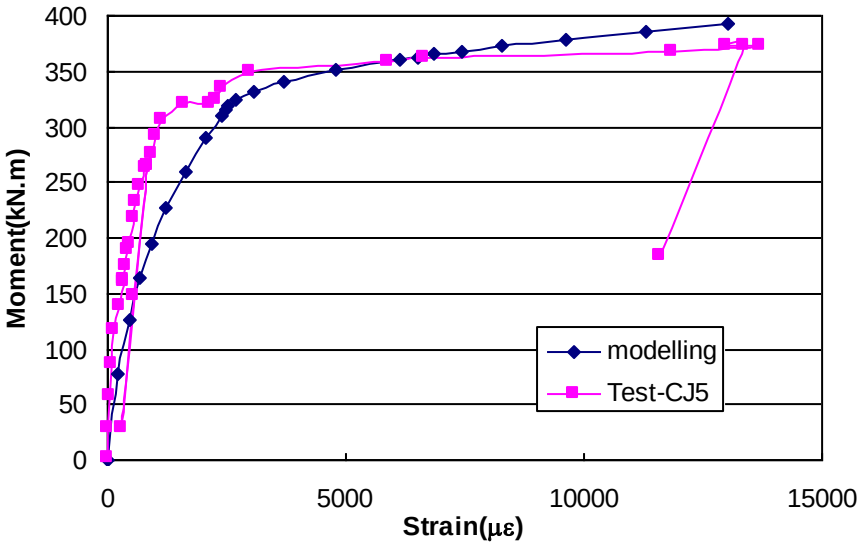

Fig 9 Moment vs. strain curves of the rebar for test CJ5 and FE-solution

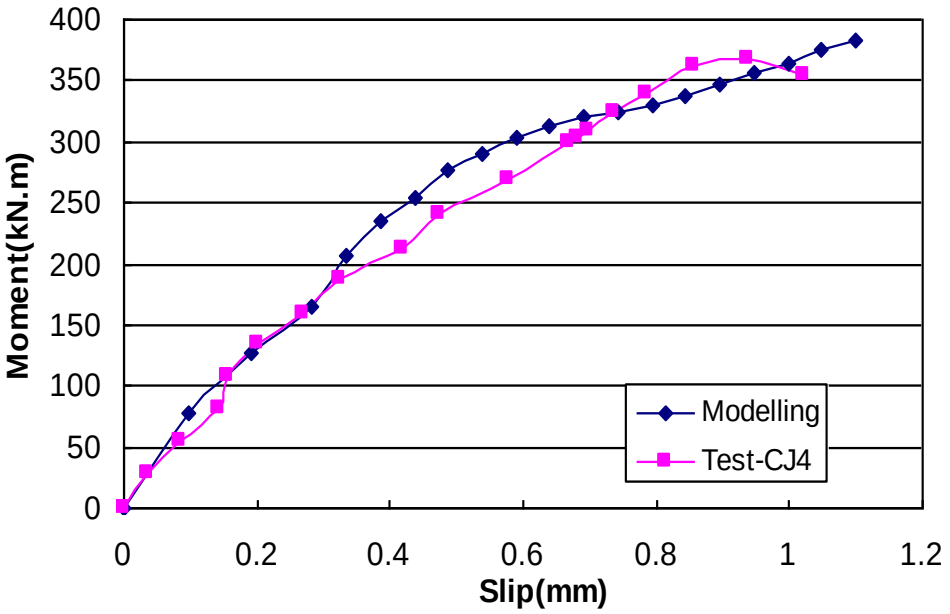

Fig 10 Comparison of moment- first stud slip curve for CJ4

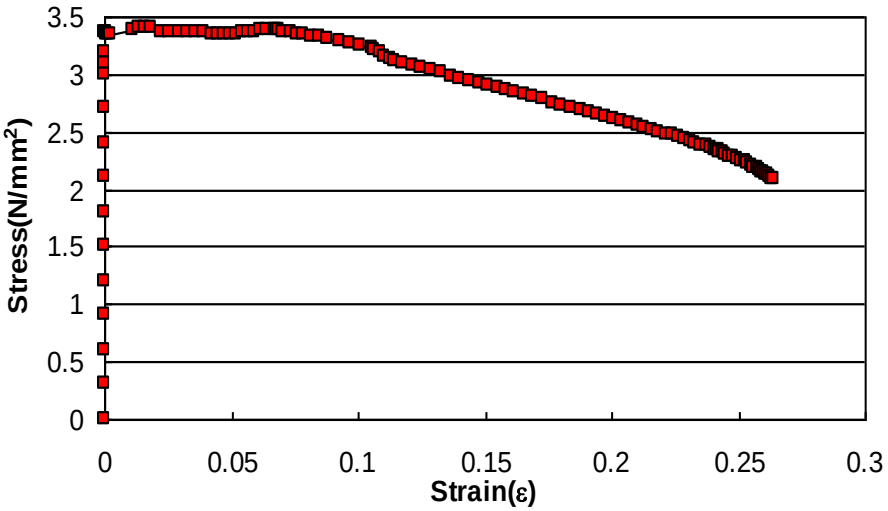

Fig 11 Typical strain-stress relationship of the concrete material of FE-solution

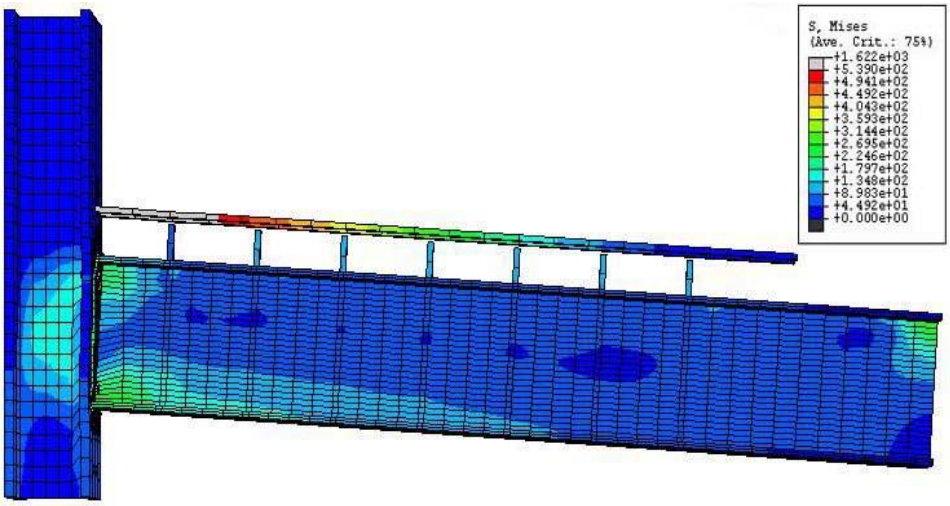

Fig. 12 CJ1 at failure (without showing the slab)

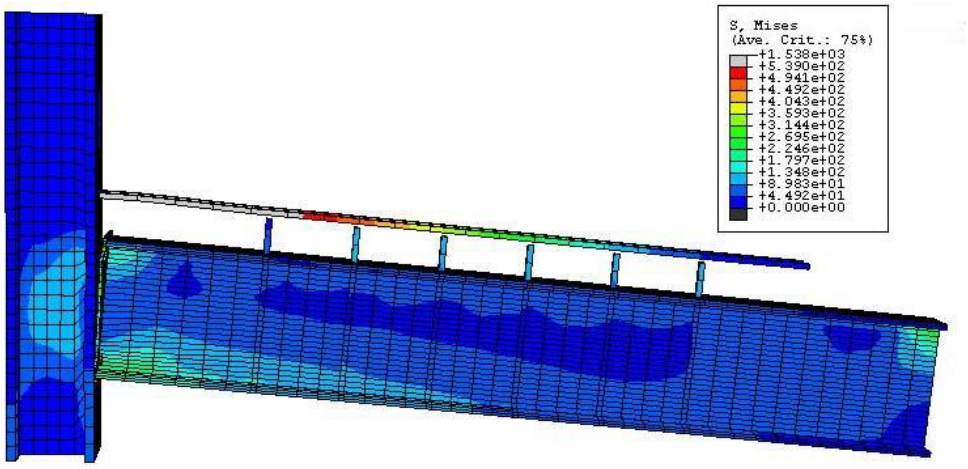

Fig 13 CJ1-6studs at failure (without showing the slab)

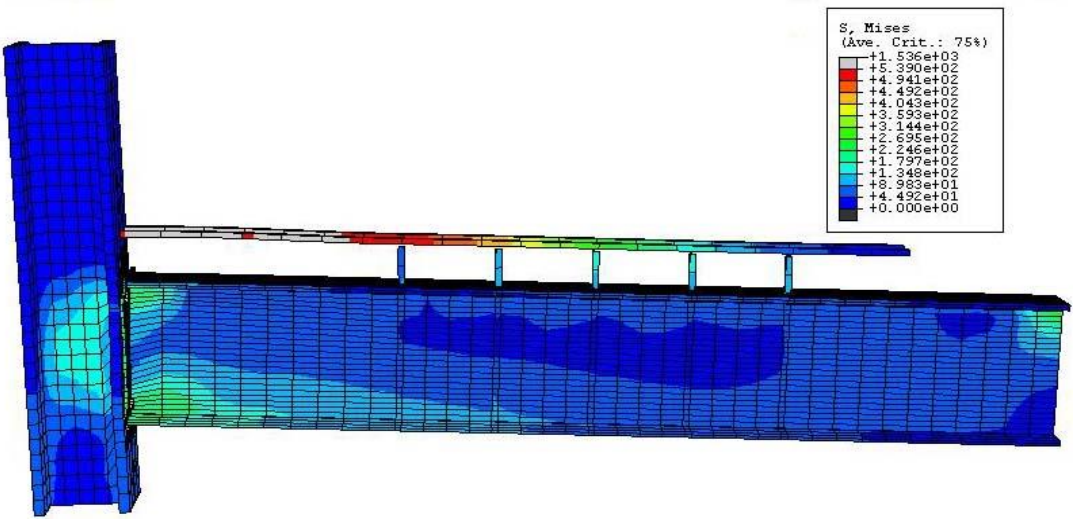

Fig.14 CJ1-5studs at failure (without showing the slab)

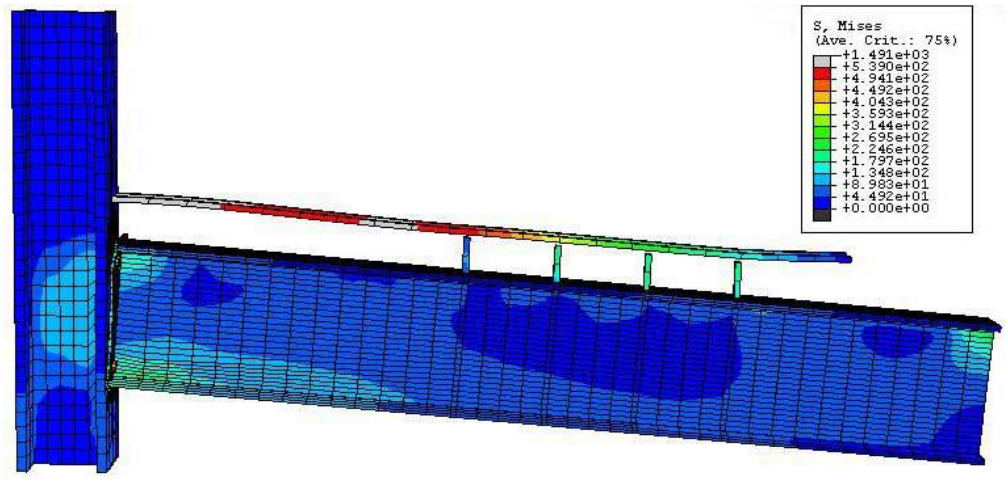

Fig.15 CJ1-4studs (without showing the slab)

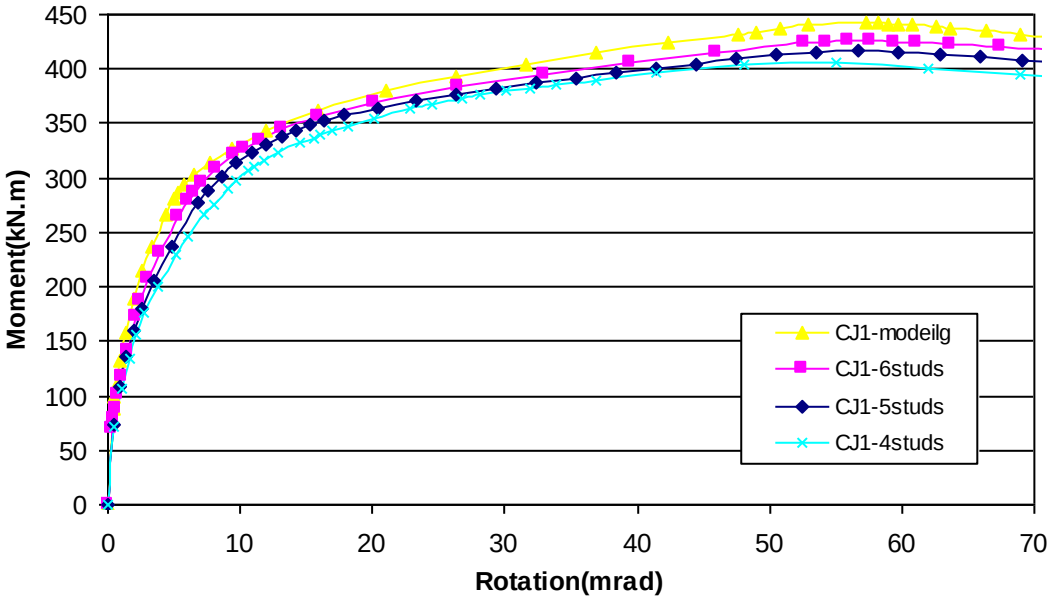

Fig.16 Variation of moment-rotation curves with different first stud spacing

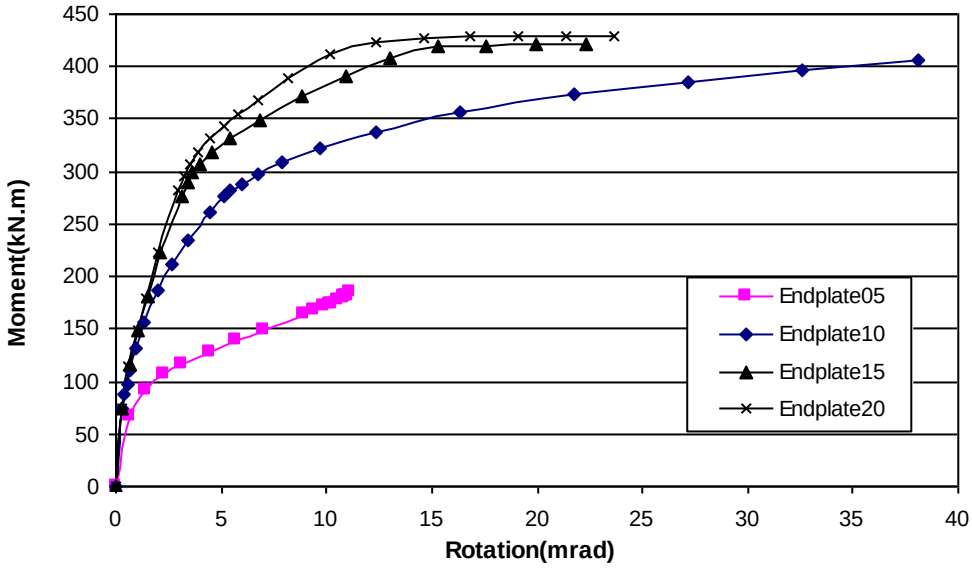

Fig. 17 Variation of moment-rotation curves with different thickness of endplate

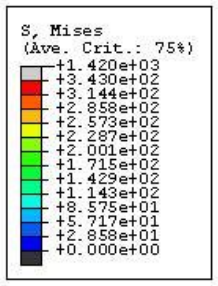

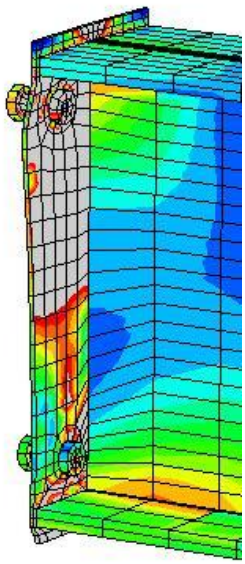

Fig.18 mode of failure of model endplate05

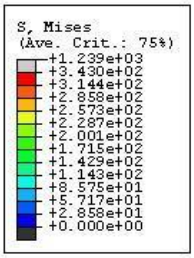

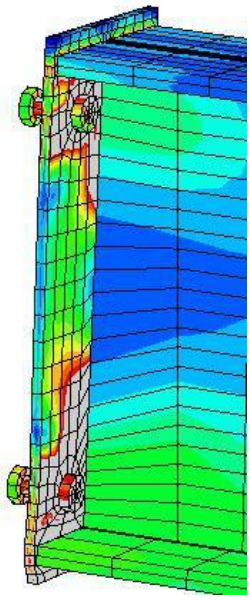

Fig.19 mode of failure of model endplate10

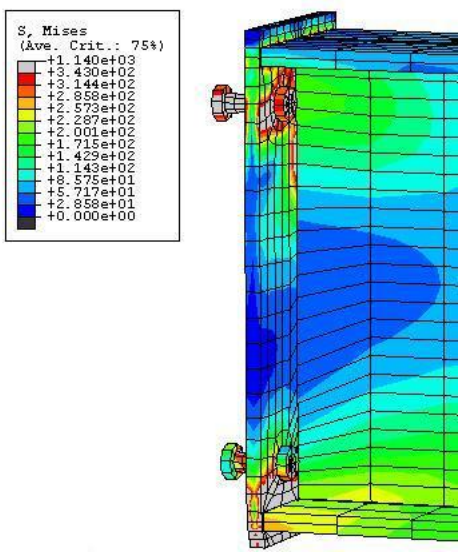

Fig.20 mode of failure of model endplate15

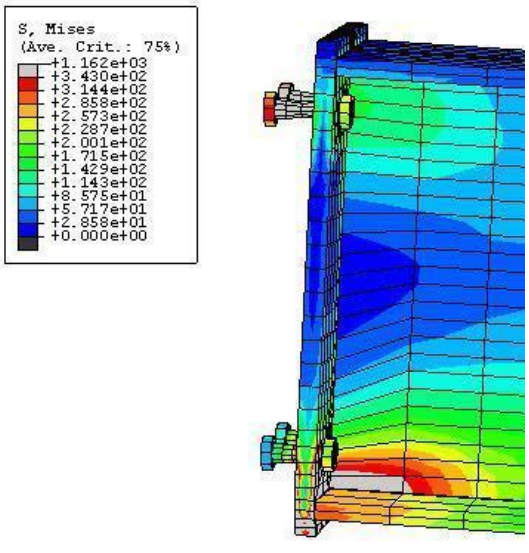

Fig.21 mode of failure of model endplate20

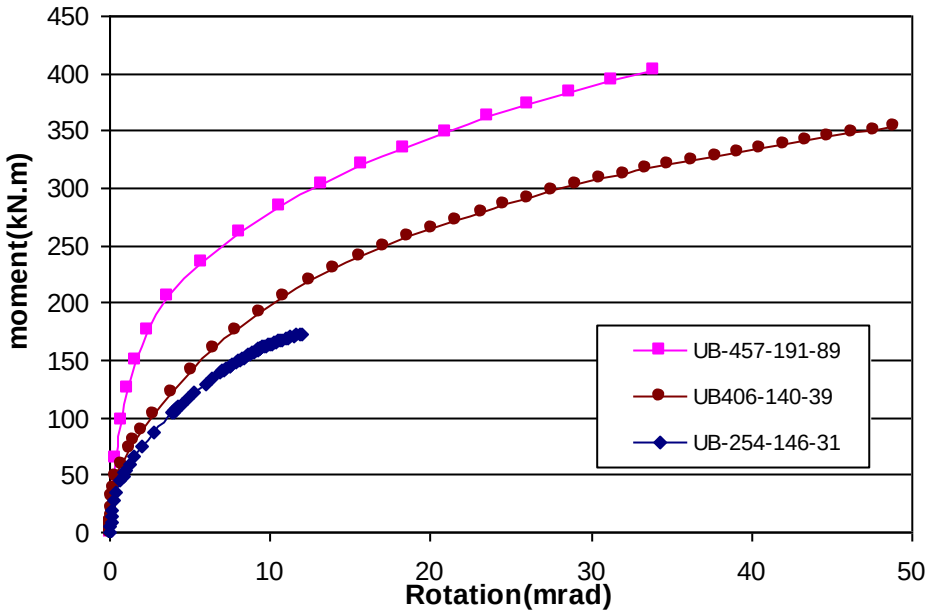

Fig.22 Variation of moment-rotation curves with different size of the beam

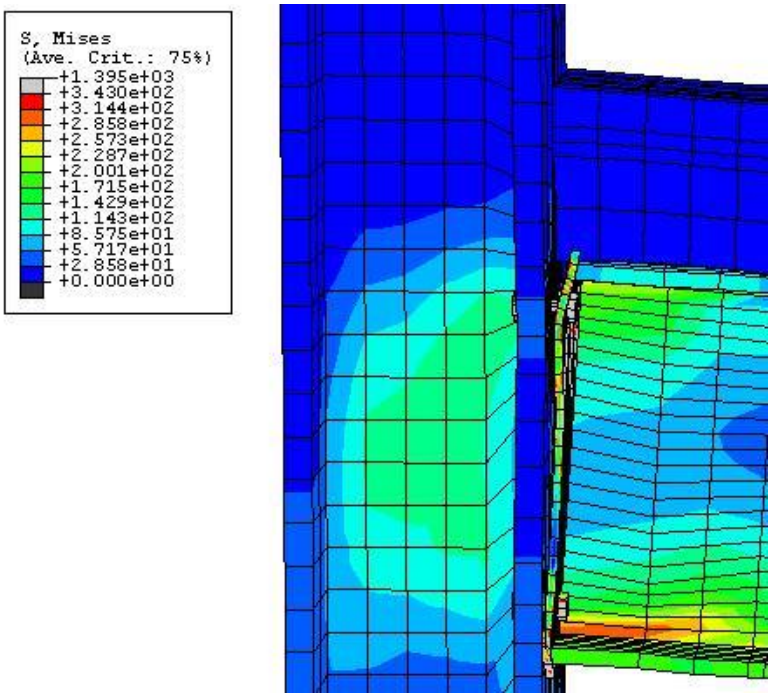

Fig.23 Model UB-457×191×89 at failure

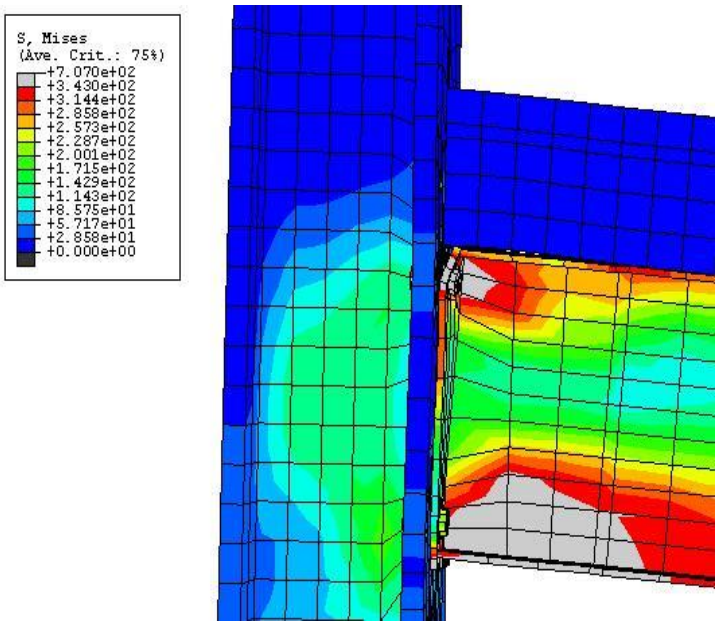

Fig.24 Model UB-406×140×39 at failure

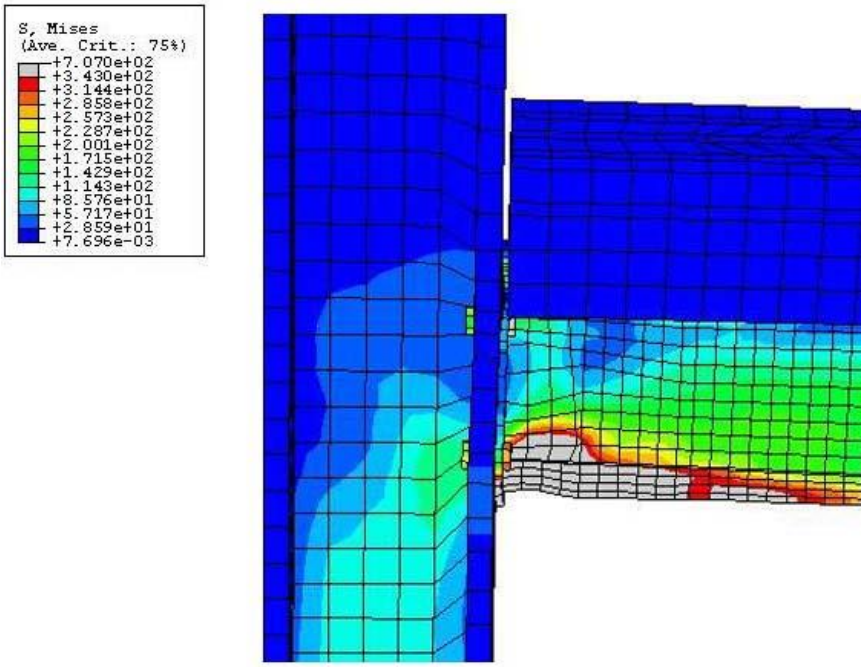

Fig.25 model UB-246-146-31 at failure

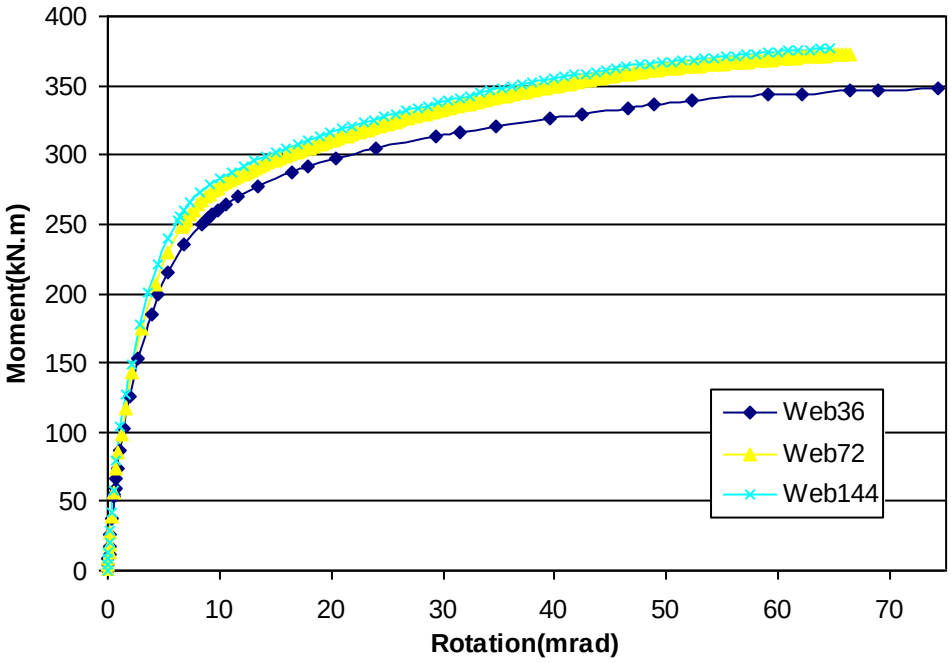

Fig.26 Variation of moment-rotation curves with different web thickness

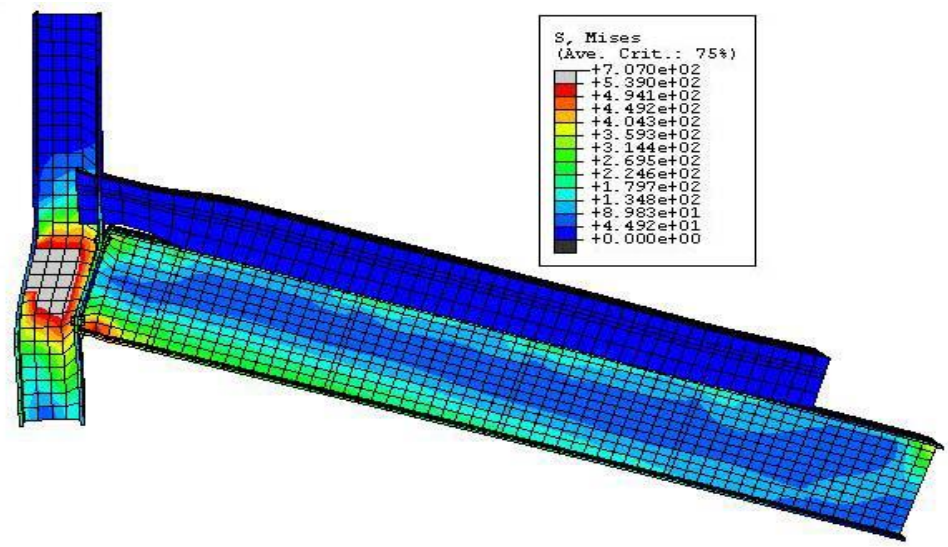

Fig.27 Model Web36 at failure

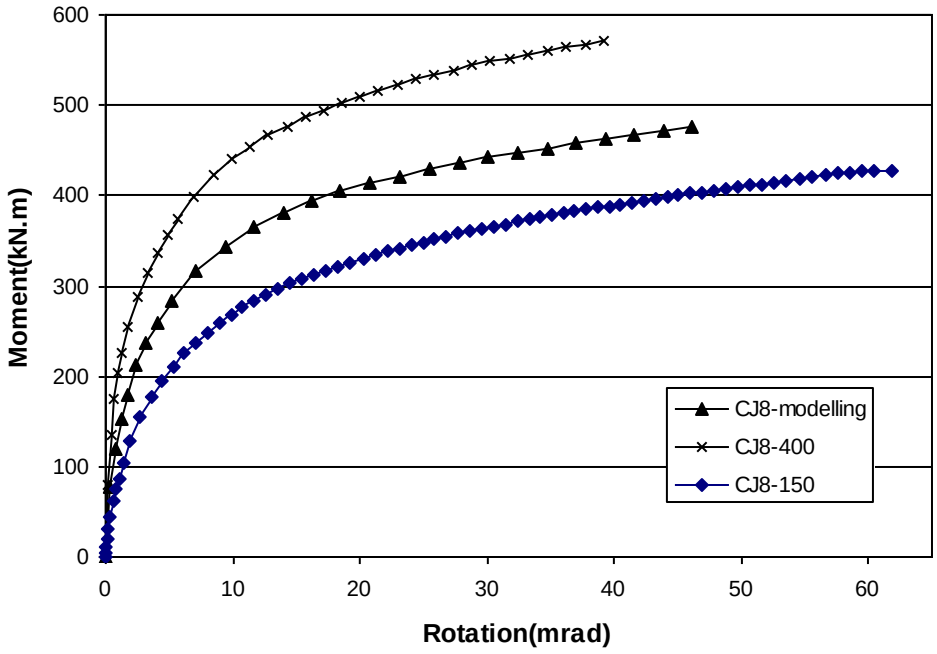

Fig.28 Variation of moment-rotation curves with different thickness of the slab